

Benford's law gives better scale exponents in phase transitions of quantum XY models

Ameya Deepak Rane, Utkarsh Mishra, Anindya Biswas, Aditi Sen(De), and Ujjwal Sen
Harish-Chandra Research Institute, Chhatnag Road, Jhansi, Allahabad 211 019, India

Benford's law is an empirical law predicting the distribution of the first significant digits of numbers obtained from natural phenomena and mathematical tables. It has been found to be applicable for numbers coming from a plethora of sources, varying from seismographic, biological, financial, to astronomical. We apply this law to analyze the data obtained from physical many-body systems described by the one-dimensional anisotropic quantum XY models in a transverse magnetic field. We detect the zero-temperature quantum phase transition and find that our method gives better finite-size scaling exponents for the critical point than many other known scaling exponents using measurable quantities like magnetization, entanglement, and quantum discord. We extend our analysis to the same system but at finite temperature and find that it also detects the finite temperature phase transition in the model. Moreover, we compare the Benford distribution analysis with the same obtained from the uniform and Poisson distributions. The analysis is furthermore important in that the high-precision detection of the cooperative physical phenomena is possible even from low-precision experimental data.

I. INTRODUCTION

Benford's law is an empirical law, based on the observation that the first significant digits, in a given set of data are not random. Instead, the chance that the first significant digit from the set of data happens to be "1" is almost 30%, "2" almost 17%, and so on. The frequency of the digit "9" is the lowest among all the digits from 1 to 9, and it is around 4.5%. The law was first observed by the astronomer Simon Newcomb in 1881 [1], who also proposed the probability function to the distribution. It is this distribution which is today known as the "Benford's Law" or "The Law of First Digit" or "The Leading Digit Phenomenon". This law was rediscovered by Frank Benford in 1938 [2]. Benford's law predicts the frequency distribution of the first significant digit D as

$$P_D = \log_{10}\left(1 + \frac{1}{D}\right). \quad (1)$$

The law has since been verified for a wide spectrum of situations in natural science, and while studying mathematical series [3]. Not all sets of numbers obey this law, e.g. random numbers obtained from a computer code will not obey such a law, and the frequency of any number from 1 to 9 as a leading digit will be $1/9$. But there are examples ranging from data obtained in earthquakes, and the brightness of gamma rays that reaches earth, to the rotation rates of spinning stars, where Benford's law is respected [3]. Violations of the law have been used in detecting cases of tax fraud, election fraud, digital image manipulation, faint earthquakes, and phase transitions [4, 5]. The scale invariance of Benford law also makes it independent of the measuring device used to get the source data [6].

A quantum phase transition (QPT) is a change in the phase of a system at zero temperature, driven by some parameter of the system, like external magnetic field or the coupling strength between particles. Unlike the thermal phase transitions [7] where the transition arises due to thermal fluctuations in the system, quantum phase

transitions are driven solely by quantum fluctuations [8]. Understanding quantum phases in many-body quantum systems is important for a number of reasons, including discerning quantumness in systems of several particles and realizing quantum computers. The one-dimensional transverse XY model is an integrable model where a quantum phase transition occurs at zero temperature when the external transverse field is varied [9–11]. This model has been studied, e.g. in crystals of CoNb_2O_6 [12]. Spectacular advances in cold gas experimental techniques in recent years have led to the possibility of experimental detection of such transitions in optical lattice systems and ion traps [13].

In this paper, we consider the anisotropic quantum XY models, in one dimension, for finite- and infinite-size systems. The system undergoes a quantum phase transition at $\lambda \equiv h/J = \lambda_c \equiv 1$, where h is the strength of the external magnetic field while J is the coupling strength between neighboring spins. Here we use the Benford's law to detect the transition and investigate its scaling properties. The main advantage of this approach is its amenability to experiments, owing to the fact that one requires to investigate only the first significant digit of an observable, which can be easily measured in experiments. We study the transverse magnetization as a function of the external magnetic field. The difference between the frequency distributions of the first significant digits of the transverse magnetization and the expected frequency distribution from Benford's law, is quantified using a parameter called the Benford violation parameter (BVP). The maxima of the derivative of the BVP with respect to the magnetic field, indicates the point of the quantum phase transition (λ_c^N), in finite size systems. Finite size scaling analysis shows that the phase transition point for finite systems (λ_c^N) approaches the critical point for infinite systems (λ_c) as $N^{-\alpha}$, where α can be as high as -2.45, and N is the number of spins. We further extend this analysis to the infinite-size quantum XY model, but at non-zero temperature. The BVP shows two crossovers in the $\lambda - \tilde{T}$ plane, as the magnetic field

is varied across the critical point, where \tilde{T} is a scaled temperature. The finite temperature quantum critical region, for unit anisotropy, is contained within the lines $\tilde{T} = -0.546(\lambda - \lambda_c)$, for $\lambda < \lambda_c$ and $\tilde{T} = 0.567(\lambda - \lambda_c)$, for $\lambda > \lambda_c$. Besides, we find that the Benford distribution is not the only distribution which can be used to detect the quantum phase transition. We show that other discrete distributions like the uniform and the Poisson (for a number of values of its parameter) can signal the QPT. We find the scaling exponents of the quantum critical point by using the uniform and the Poisson distributions. We also analyze the effect of changing the distance measure between the observed and predicted probability distributions on the scaling exponents. The distance measures used here are mean deviation, standard deviation, and the Bhattacharya metric [14]. We find that the analyses using the Benford distribution, in general, provide higher values of the scaling exponents.

The paper is organized as follows. In Sec. II, we briefly discuss the one-dimensional quantum XY models for both finite and infinite systems. Sec. III contains a discussion on the methodology and tools used in the analysis of the data. The detection of phase transition by using the BVP of transverse magnetization and the scaling of quantum critical point for finite size systems is discussed in Sec. IV. Further analysis of the phase space diagram in the finite temperature case for infinite systems is taken up in Sec. V. In Sec. VI, we show that the uniform and the Poisson distributions can also be used to detect a QPT. We compare the results with the ones obtained using the Benford distribution. Finally, we conclude in Sec. VII.

II. DESCRIPTION OF THE MODEL

The Hamiltonian of the one-dimensional anisotropic quantum XY model is given by

$$H = \frac{J}{2} \sum_{i=1}^N [(1 + \gamma)\sigma_i^x \sigma_{i+1}^x + (1 - \gamma)\sigma_i^y \sigma_{i+1}^y] + h \sum_{i=1}^N \sigma_i^z \quad (2)$$

where J is the coupling constant, h is the strength of the transverse magnetic field, $\gamma (\neq 0)$ is the anisotropy parameter, and σ 's are the Pauli matrices in a system of N quantum spin-1/2 particles. We assume periodic boundary condition. The system undergoes a quantum phase transition from long range antiferromagnetic to paramagnetic phase at $h/J = 1$ [9–11]. The model is diagonalizable by applying successive Jordan-Wigner, Fourier, and Bogoliubov transformations [9–11]. The average transverse magnetization can be calculated for any number of spins at any temperature. The anisotropic quantum XY models for $\gamma \neq 0$ forms the ‘‘Ising universality class’’. For $\gamma = 1$, the Hamiltonian described by Eq. (2) is known as the Ising Hamiltonian. For finite spin systems, the trans-

verse magnetization reads

$$M_z(\lambda, \tilde{\beta}, N) = -\frac{2}{N} \sum_{p=1}^{N/2} \frac{\tanh(\tilde{\beta}\Lambda(\lambda)/2)(\cos(\phi_p) - \lambda)}{\Lambda(\lambda)}, \quad (3)$$

where $\beta = \frac{1}{kT}$, k is the Boltzmann constant, T is the absolute temperature, $\tilde{\beta} = \beta J$, $\phi_p = \frac{2\pi p}{N}$, and $\Lambda(x) = \{\gamma^2 \sin^2(\phi_p) + [x - \cos(\phi_p)]^2\}^{1/2}$, while for infinite systems, the transverse magnetization is given by

$$M_z(\lambda, \tilde{\beta}) = -\frac{1}{\pi} \int_0^\pi d\phi \frac{\tanh(\tilde{\beta}\Lambda(\lambda)/2)(\cos(\phi) - \lambda)}{\Lambda(\lambda)} \quad (4)$$

where $\Lambda(x) = \{\gamma^2 \sin^2(\phi) + [x - \cos(\phi)]^2\}^{1/2}$. The two site correlation functions can also be calculated analytically for this model for both finite and infinite lattice sizes at any temperature. The nearest neighbor diagonal correlations can be expressed in terms of a correlator, $G(R, \lambda)$, through

$$C_{xx}(\lambda) = G(-1, \lambda), C_{yy}(\lambda) = G(1, \lambda), \quad (5)$$

and

$$C_{zz}(\lambda) = [M_z(\lambda)]^2 - G(-1, \lambda)G(1, \lambda), \quad (6)$$

where $G(R, \lambda)$, for infinite lattice size and zero temperature, is given by

$$G(R, \lambda) = \frac{1}{\pi} \int_0^\pi d\phi \frac{(\gamma \sin(\phi R) \sin(\phi) - \cos(\phi)(\cos(\phi) - \lambda))}{\Lambda(\lambda)}. \quad (7)$$

III. BENFORD VIOLATION PARAMETER: THE METHODOLOGY

We now discuss the methodology employed to analyze the data obtained for a given observable by using the Benford violation parameter. The idea of the Benford violation parameter is to characterize an observable in terms of the frequencies of the first significant digits. To do this, we compare it with the expected Benford frequency, and quantify it with a number, which we call the Benford violation parameter.

A. Computing the BVP

For an observable $Q(x)$, defined in a range $[a, b]$ of x , we sample N points in the range. Let us denote the minimum and maximum values of the observable in a subinterval $[a', b']$ comprising of n points, of the total interval $[a, b]$, by Q_{\min} and Q_{\max} respectively. Using these two values, we create a set of data for the observable, such that all the values in $[a', b']$ lie in the range $[0, 1]$ [5]. The

new value of Q , “Benford Q ”, is denoted by Q^B , and is given by

$$Q^B = \frac{Q - Q_{\min}}{Q_{\max} - Q_{\min}}. \quad (8)$$

The frequency of the first significant digit to be D , obtained from these new values, is called the “observed” frequency, O_D , for $D=1,\dots,9$. Note that the procedure given in Eq. (8) is important to obtain a nontrivial frequency distribution of digits from 1 to 9. The rescaling is necessary, since a distribution varying between 1 and 2, for example, will never have the first significant digit larger than 2. The next step is to compare O_D with the expected frequency distribution given by Benford’s law, denoted by $E_D = n \log_{10}(1 + \frac{1}{D})$. So, for any observable Q , we denote the violation parameter by $\delta(Q)$, and define it as

$$\delta(Q) = \sum_{D=1}^9 \left| \frac{O_D - E_D}{E_D} \right|. \quad (9)$$

This number gives us the variation of the observable with respect to the Benford frequency and we assign this number to the mid-point of the range $[a', b']$. The subinterval $[a', b']$ determines the error of the variable x . Therefore, it should be small compared to the range of the total interval $[a, b]$. The number of data points n in this subinterval should be large enough to ensure convergence of the BVP. Note that, lower the value of $\delta(Q)$, better is the distribution’s conformity with the Benford’s law.

IV. BENFORD SCALING OF QUANTUM PHASE TRANSITION IN THE TRANSVERSE XY MODEL

In this and the succeeding two sections, we present our main findings regarding the BVP and quantum phase transition in the quantum XY model. The current section deals with the zero temperature behavior, while the succeeding one is for the finite-temperature regime. In the zero temperature case, we first show that the BVP of the transverse magnetization and correlations are able to detect the QPT in this model. We subsequently perform a finite-size scaling analysis on the BVP data of the system, which indicates the possibility of detecting the QPT in finite-sized systems, potentially realized in cold gas experiments. We show that the scaling exponent obtained by using the BVP of M_z is much higher than the ones obtained by using M_z itself and several other physical quantities. The analysis points to the following interesting possibility. By using the BVP as an order parameter, a QPT can be detected with high-precision even in finite-sized systems, and even in cases where the observables can be measured in the experiment with a low precision.

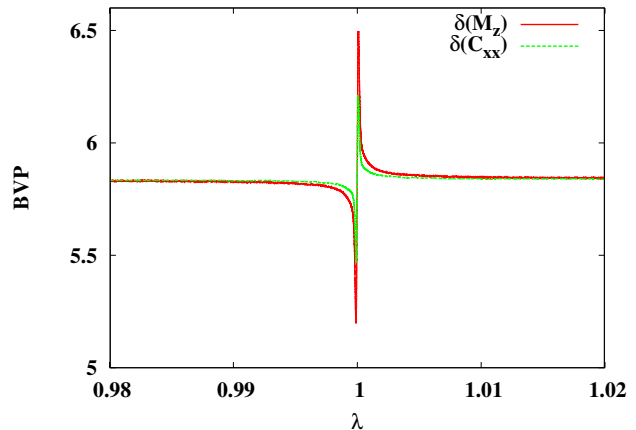


FIG. 1. (Color online.) The BVP for M_z and C_{xx} for the infinite quantum Ising model. There is an abrupt change in the BVP at the QPT point. The axes are dimensionless. The features remain similar for any $\gamma \neq 0$.

A. Detection of QPT

We now compute the BVP for M_z and C_{xx} for the infinite quantum XY model. The basic idea involved in Benford analysis for any observable was discussed in the preceding section. To obtain the Benford magnetization, M_z^B , for a given value of the driving parameter λ , we choose a small interval around λ of width ϵ , $(\lambda - \epsilon/2, \lambda + \epsilon/2)$, where ϵ is a small number. In this small interval, we choose n values of the system parameter, λ . Corresponding to those n values of the field, we get n values for the transverse magnetization of the system from Eq. (4). From this set of data for magnetization, the normalized Benford transverse magnetization is obtained by using Eq. (8). To get the violation parameter for M_z , we then find the corresponding O_D ’s and subsequently use Eq. (9). The same analysis is performed in the entire range of λ . The entire procedure is repeated for the calculation of BVP of C_{xx} . We find that away from the quantum critical point ($\lambda_c = 1$), the BVP is almost constant and changes little as we change λ (see Fig. 1). However, as we move towards the quantum phase transition, we see a very sharp transverse movement in the BVP at $\lambda_c = 1$. From Fig. 1, it can be seen that the BVP of both M_z and C_{xx} detect the quantum phase transition in the model. We have checked that the BVP of other two-site correlators, including two-site entanglement, can also detect the QPT in this model.

B. Finite-size scaling

By virtue of the current advances in cold gas experimental techniques, one can now engineer finite quantum spin systems in laboratories [13]. It is therefore impor-

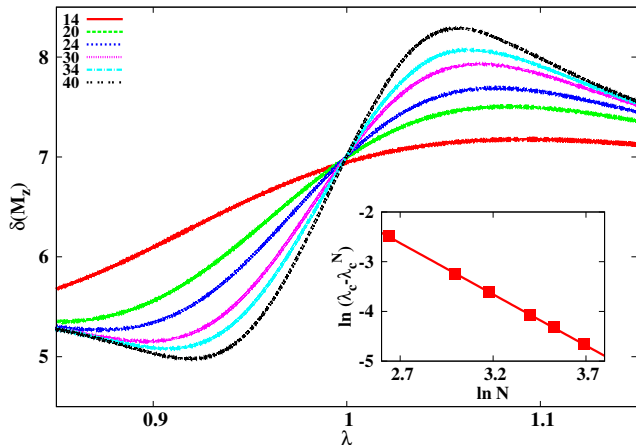


FIG. 2. (Color online.) BVP of transverse magnetization, $\delta(M_z)$, with respect to the external magnetic field, with the legends indicating the number of spins. The violation of Benford's law increases as one moves from the magnetically ordered state for $\lambda < \lambda_c$, to the paramagnetic state for $\lambda > \lambda_c$. The inset shows the scaling of the critical point (λ_c^N) with the system size N . The data points for the figure in the inset are obtained by using the method illustrated in Fig. 3, to get the maximum in the derivative of $\delta(M_z)$ with respect to λ . The critical point λ_c^N approaches λ_c as $N^{-2.06}$. All axes are dimensionless, except the horizontal one in the inset, which is in \ln of the number of spins. The plots and the results are for $\gamma = 0.5$, which remains similar any $\gamma \neq 0$.

tant to study the QPT point and its scaling with increasing system sizes for finite systems. In our finite-size analysis, we have taken the range of λ to be $[0.8, 1.2]$ (see Fig. 2). The plot shows the BVP as a function of λ for different system sizes. We have considered systems of finite (periodic) chains consisting of N spins, with $N = 14, 20, 24, 30, 34, 40$. The convergence of the BVP is ensured by taking a sufficient number of sample points in each subinterval of λ . Note that the BVP has a large transverse movement around the quantum critical point. The variation of Benford magnetization with λ is similar to the variation of transverse magnetization itself with λ around the QPT. It can be readily seen from Fig. 2 that the derivative of Benford magnetization with λ will peak at the point of QPT, as the curvature of the BVP changes from concave to convex there. Therefore, it is important to find the derivative of BVP with respect to λ . The curves in Fig. 2 look quite smooth from a distance, but a closer inspection reveals fluctuations in the curves. However, it is quite evident that the curvatures of the curves change from concave to convex, around the point of QPT. Four fixed points are required to draw such a curve. Therefore, we fit a cubic polynomial to the data for BVP in the appropriate range of λ , for a fixed N , using the method of least squares and find the exact point where the derivative has a maximum. The value of λ corresponding to this maxima is the predicted point of QPT for the partic-

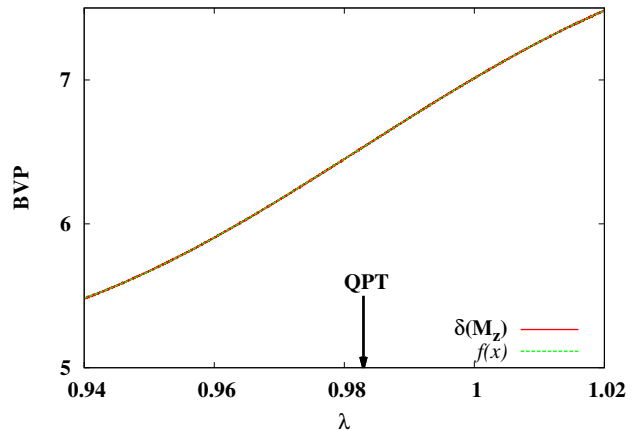


FIG. 3. (Color online.) A cubic polynomial $f(x)$ is fitted to $\delta(M_z)$, for $N = 30$, in the appropriate range of λ , using the method of least squares. The constants of $f(x)$ have an error of the order of 0.02%. The point of QPT, marked in the figure at $\lambda = 0.9830$, is predicted in this finite system for the considered order parameter, and corresponds to the maxima of $f'(x)$. All axes are dimensionless. Note that the two curves, for $\delta(M_z)$ and $f(x)$ have merged with each other. Here, $\gamma = 0.5$.

ular system size N and the particular order parameter considered. We denote this value of λ by λ_c^N . We have performed this analysis for $N = 14, 20, 24, 30, 34, 40$. In Fig. 3, we present a summary of this analysis for $N = 30$. In the inset of Fig. 2, we plot $\ln(\lambda_c - \lambda_c^N)$ with respect to $\ln N$. We find that a straight line fits the plot, which we find via the method of least squares. Exponentiating the equation of the straight line, for $\gamma = 0.5$, we obtain that λ_c^N approaches λ_c as $N^{-2.06}$ i.e.

$$\lambda_c^N = \lambda_c + kN^{-2.06}. \quad (10)$$

The error associated with the estimation of the scaling exponent is of the order of 0.5%. The scaling exponent found using the Benford magnetization is much higher than many other known scaling exponents for this model. In particular, the scaling exponents for transverse magnetization, fidelity, concurrence, quantum discord, and shared purity are significantly lower [7, 15–17]. In Fig. 4, we plot the scaling of the critical point λ_c^N with N for three values of the anisotropy parameter γ . The scaling exponents for $\gamma = 0.1, 0.5$, and 1.0 are $-2.14, -2.06$, and -2.10 respectively.

Note that the procedure for Benford analysis described in this paper is not unique. We compare two frequency distributions, one of which is obtained from Benford's law and the other is obtained theoretically or experimentally from a natural phenomenon. The distance between the two distributions is quantified by a number obtained by using a measure. The choice of this measure is not unique. We have reported the results until now by using the mean deviation as our distance measure. But now we also use the standard deviation and the Bhat-

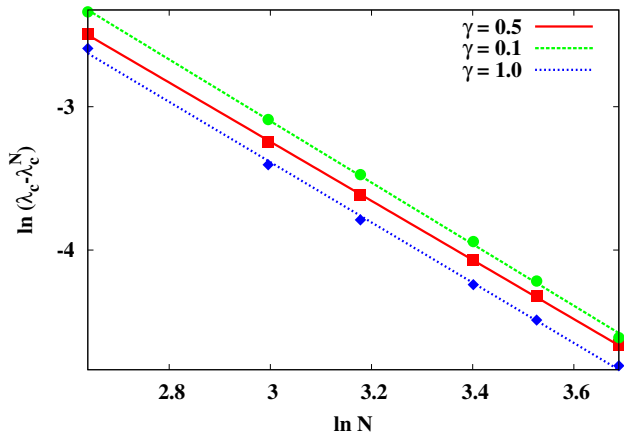


FIG. 4. (Color online.) The scaling of the critical point λ_c^N with N for three values of the anisotropy parameter. The scaling exponents for $\gamma = 0.1, 0.5$, and 1.0 are $-2.14, -2.06$, and -2.10 respectively. Note that the lines are almost parallel to each other. The vertical axis is dimensionless, while the horizontal one is in \ln of the number of spins.

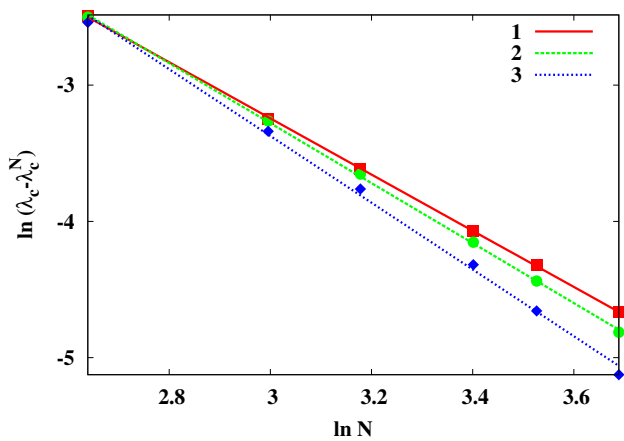


FIG. 5. (Color online.) The scaling of the critical point λ_c^N with N . The Benford distribution has been used in conjunction with the mean deviation (1), standard deviation (2), and Bhattacharya distance (3), to analyze the data for transverse magnetization. The scaling exponents for (1), (2), and (3) are $-2.06, -2.20$, and -2.45 respectively. The vertical axis is dimensionless, while the horizontal one is in \ln of the number of spins. Here, $\gamma = 0.5$.

tacharya metric [14] to quantify the distance between two frequency distributions. So, for any observable Q , we define the violation parameter $\delta(Q)_{sd}$, using the concept of standard deviation, as

$$\delta(Q)_{sd} = \frac{1}{3} \sqrt{\sum_{D=1}^9 (O_D - E_D)^2}. \quad (11)$$

The violation parameter $\delta(Q)_{Bd}$, corresponding to the

Bhattacharya metric, can be defined as

$$\delta(Q)_{Bd} = -\ln \sum_{D=1}^9 \sqrt{O_D E_D}. \quad (12)$$

We observe that the Benford distribution, combined with any of these measures, to discriminate the observed and expected frequency distributions, applied to data obtained for M_z or C_{xx} , can be used to detect the QPT point for the infinite quantum XY model. We extend the analysis to finite-sized systems and obtain the scaling exponents. In Fig. 5, we plot the scaling of the critical point λ_c^N with N , using the Benford distribution in conjunction with the mean deviation, standard deviation, and the Bhattacharya distance, to analyze the data for transverse magnetization. We find that the scaling exponents are affected by the choice of the measure quantifying the violation parameter. The scaling exponents, for $\gamma = 0.5$, obtained by using the mean deviation, standard deviation, and the Bhattacharya distance are $-2.06, -2.20$, and -2.45 respectively. This shows that the Bhattacharya metric provides a better scaling among the considered metrics for the Benford distribution.

V. PHASE TRANSITION AT FINITE TEMPERATURE

In this section, we discuss the finite temperature phase transition in the quantum XY model. A quantum phase transition is a phase transition at zero temperature driven by quantum fluctuations. But zero temperature is a theoretical concept which cannot be reached in experiments. However, current cooling methods enable one to reach temperatures of a few nanoKelvin. Therefore, it is important to study the status of the phase transition considered in the preceding section at very low temperatures, in the presence of both quantum and thermal fluctuations. In the finite temperature quantum XY model, the system crosses over from the magnetically ordered region to the quantum critical region and then to the paramagnetic region as the field is varied at a fixed finite temperature [8, 18, 19].

We consider an infinite system at a finite but very low temperature. The transverse magnetization of the system is calculated using Eq. (4) as a function of the driving parameter and temperature. In Fig. 6, we plot the projection of the partial derivative of transverse magnetization with respect to temperature, $\partial M_z(\lambda, \tilde{T})/\partial \tilde{T}$, in the $\lambda - \tilde{T}$ plane, where $\tilde{T} = kT/J$, for $\gamma = 1$. The positions of the maxima (yellow) for $\lambda < \lambda_c$ and minima (white) for $\lambda > \lambda_c$ form the phase transition lines in the $\lambda - \tilde{T}$ plane. Note that the temperature is a linear function of the driving parameter at such low temperatures, along the lines of phase transition. In an effort to investigate the Benford approach further and compare it with the established methods of data analysis, like the derivative method given above, we analyze the finite temperature

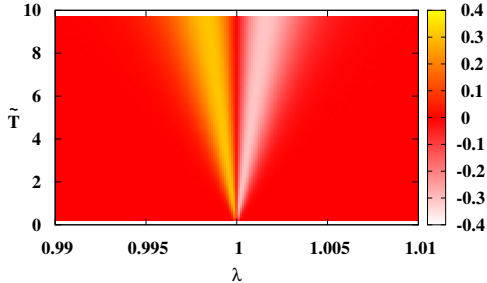


FIG. 6. (Color online.) Projection of the derivative of transverse magnetization with respect to temperature, $\partial M_z(\lambda, \tilde{T})/\partial \tilde{T}$, on the $\lambda - \tilde{T}$ plane. The \tilde{T} axis plotted is multiplied by 10^4 . The positions of the maxima (yellow) for $\lambda < \lambda_c$ and minima (white) for $\lambda > \lambda_c$ form the phase transition lines in the $\lambda - \tilde{T}$ plane. All quantities plotted are dimensionless. Here, $\gamma = 1$.

data using Benford’s law. We calculate the BVP of transverse magnetization ($\delta(M_z)$), as a function of the driving parameter for a set of fixed temperatures close to absolute zero. The data obtained turns out to be very similar to that plotted in Fig. 6 with $\partial M_z(\lambda, \tilde{T})/\partial \tilde{T}$ replaced by $\delta(M_z)$. We plot the exact positions of the maxima and minima on the two panels shown in Fig. 7, which turn out to be almost identical. It can be seen that the system undergoes two phase transitions at any fixed finite temperature as the driving parameter is varied. Straight lines are fitted to the obtained data using the method of least squares. The cross-over lines obtained by using the Benford analysis, for $\gamma = 1$, are given by the equations

$$\begin{aligned} \tilde{T} &= -0.546(\lambda - \lambda_c), & \lambda < \lambda_c \\ \tilde{T} &= 0.567(\lambda - \lambda_c), & \lambda > \lambda_c. \end{aligned} \quad (13)$$

The errors associated with the values of the constants in these equations are of the order of 1%. We therefore find that just like for the zero temperature case, the finite temperature transitions are also easily detected by the experimentally less-demanding Benford analysis.

VI. COMPARISON WITH OTHER DISTRIBUTIONS

Let us now revert back to the zero-temperature regime. Since the BVP detects the QPT point, it is natural to ask if the Benford distribution is the only one that is capable of detecting the quantum critical point in the quantum XY model. Therefore, we investigate the problem using a few other discrete frequency distributions. The simplest frequency distribution is the uniform distribution. The frequency of the first significant digit “ D ” of the uniform

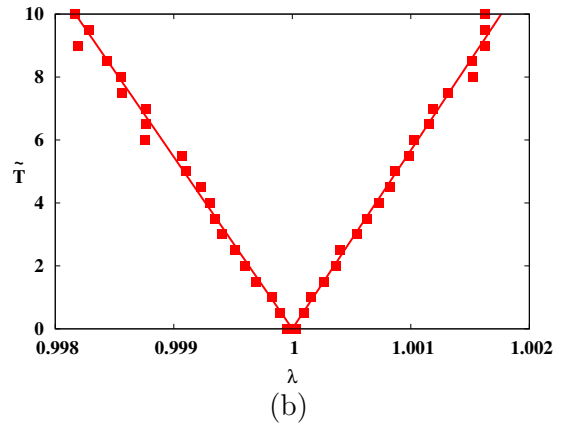
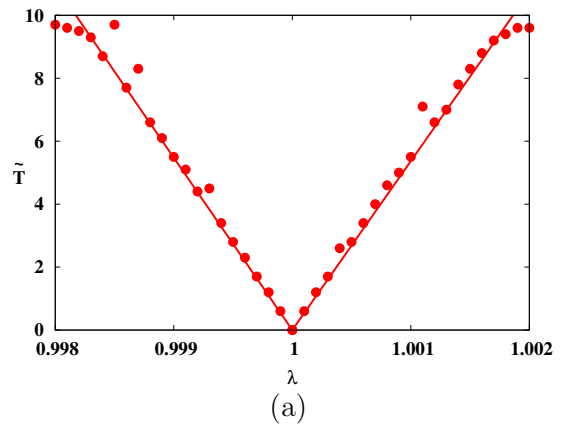


FIG. 7. (Color online.) The cross-over lines are plotted in the $(\lambda - \tilde{T})$ plane. The plots clearly show two phase transitions at finite temperatures at two critical values of the driving parameter. The positions of the maxima and minima are plotted for $\partial M_z(\lambda, \tilde{T})/\partial \tilde{T}$ in panel (a), and for BVP of transverse magnetization ($\delta(M_z)$) in panel (b). All quantities plotted are dimensionless. The \tilde{T} -axes plotted are multiplied by 10^4 . The results are for the Ising model ($\gamma = 1$), but they remain similar for any $\gamma \neq 0$.

distribution is given by

$$P_D = \frac{1}{9}. \quad (14)$$

The other discrete distribution that we consider is the Poisson distribution. The frequency of the first significant digit “ D ” of the Poisson distribution is given by

$$P_D = \frac{\kappa^D e^{-\kappa}}{D!} \cdot \frac{1}{N_0}, \quad (15)$$

where the parameter $\kappa > 0$. We normalize the distribution by N_0 , in such a way that $\sum_{D=1}^9 P_D = 1$. In Fig. 8, we plot the different frequency distributions. Note that for $\kappa = 1$, the Poisson distribution is qualitatively similar to the Benford distribution, while for $\kappa = 10$, the Poisson distribution is qualitatively similar to the mirror image of the Benford distribution along the $D = 5$ axis.

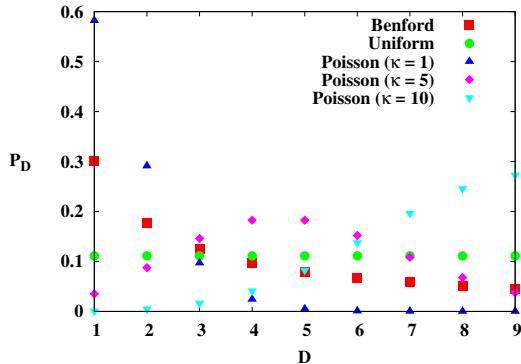


FIG. 8. (Color online.) Frequency of the first significant digits for the different normalized discrete distributions. Both axes are dimensionless.

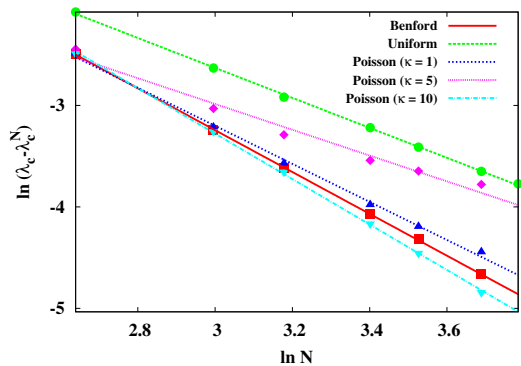


FIG. 9. (Color online.) The scaling of the critical point λ_c^N with N . The indicated frequency distributions have been used in conjunction with the mean deviation to analyze the data for transverse magnetization. The scaling exponents, for $\gamma = 0.5$, using the Benford, uniform, and Poisson ($\kappa = 1, 5, 10$) are -2.06, -1.48, -1.88, -1.27, and -2.24 respectively. The dimensions are as in Fig. 5.

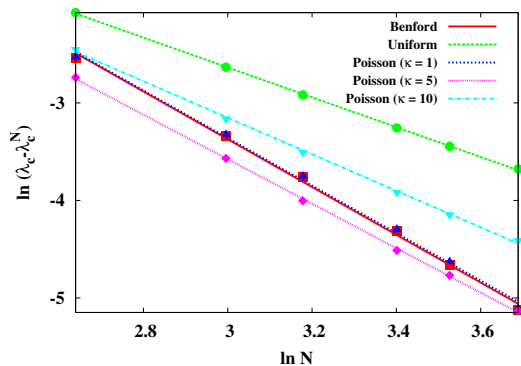


FIG. 10. (Color online.) The scaling of the critical point λ_c^N with N . The indicated frequency distributions have been used in conjunction with the Bhattacharyya distance to analyze the data for transverse magnetization. The scaling exponents, for $\gamma = 0.5$, using the Benford, uniform, and Poisson ($\kappa = 1, 5, 10$) are -2.45, -1.53, -2.44, -2.28, and -1.87 respectively. The dimensions are as in Fig. 5.

The Poisson distribution is bell-shaped for $\kappa = 5$. Now, we analyze the theoretical data using the uniform, and the Poisson distributions for $\kappa = 1, 5, 10$. We find that any of these distributions in conjunction with any of the three measures, viz. the mean deviation, the standard deviation, or the Bhattacharyya distance, when applied to theoretical data for M_z or C_{xx} in the infinite quantum XY model, detects the QPT point. However, the signatures of QPT, obtained by using the different distributions for data analysis, are different. While a minimum of the violation parameter is obtained for the uniform distribution (at the QPT), a minimum or a maximum in the derivative of the violation parameter is obtained for the other distributions. This signature is independent of the measure used in the analysis. The data analysis technique is further explored by performing finite-size scaling analysis using the data for transverse magnetization for all the different frequency distributions using the mean deviation and the Bhattacharyya distance. We present the results for $\gamma = 0.5$. However, the results are qualitatively similar for any $\gamma \neq 0$. In Fig. 9, we plot the scaling of the critical point λ_c^N with N using all the frequency distributions discussed, in conjunction with the mean deviation. We find that the choice of the frequency distribution affects the scaling exponents. The Poisson distribution with $\kappa = 10$ gives the highest scaling exponent of -2.24. The scaling exponents obtained by using the Benford, uniform, and Poisson ($\kappa = 1, 5$) distributions are -2.06, -1.48, -1.88, and -1.27 respectively. In Fig. 10, we plot the scaling of the critical point λ_c^N with N , again using all the frequency distributions, but now, in conjunction with the Bhattacharyya distance. The scaling exponents obtained using the Benford, uniform, and Poisson ($\kappa = 1, 5, 10$) distributions are -2.45, -1.53, -2.44, -2.28, and -1.87 respectively. Note that the scaling exponents obtained using the Benford distribution is among the higher ones for any measure and for any distribution. Therefore, while the procedure for data analysis involving the Benford's law is not unique, there seems to be some evidence that it is one of the better ones, if not the best that can be employed to analyze the given data.

VII. CONCLUSION

The Benford's law seems to be a very efficient tool in analyzing data. Our data analysis and subsequent results, for a quantum mechanical system reinforces the belief. We find that the quantum phase transition in the one-dimensional anisotropic quantum XY models, are efficiently detected by this analysis. The main advantage of this technique is its dependence on only the first significant digit of an observable. This advantage is very important from the point of view of experiments, in which accuracy is not very high.

We have used a number of other discrete frequency distributions along with three different measures to discriminate between frequency distributions. It is seen that

the Benford distribution is not unique and that other distributions can also be employed to analyze data and detect a quantum critical point in the quantum XY models. However, analysis of data using the Benford distribution produces higher scaling exponents in almost all cases. This indicates that this is possibly a better tool for data analysis. In this paper, we have compared pairs of frequency distributions, one of which is obtained from quantum theory and the other is obtained from a probability distribution. The distance between the two distributions is quantified by a number obtained by using a measure. The choice of this measure is not unique. We have reported our results by using the mean deviation, standard deviation, and the Bhattacharya metric to

quantify the distance between the two frequency distributions. The analysis has been carried out for both finite and infinite size systems for different observables at zero and finite temperatures. Interestingly, most of the finite size scaling exponents obtained in this paper by using the violation parameters are much higher than those obtained using other measures like magnetization, fidelity, concurrence, shared purity, and quantum discord. We also find the linear relationship between temperature and the driving parameter at a finite temperature, along the cross-over lines, in this model. The analysis strongly suggests that measuring the Benford violation parameter in the laboratory can be an efficient tool for detecting phase transitions in quantum many-body systems.

-
- [1] S. Newcomb, *Am. J. Math.* **4**, 39 (1881).
 [2] F. Benford, *Proc. Am. Phil. Soc.* **78**, 551 (1938).
 [3] There is a website that maintains a record of the works on the Benford's law at <http://www.benfordonline.net/list/chronological>.
 [4] B. Busta and R. Sundheim, Center for Business Research Working Paper No. W93-106-94, St. Cloud State University, Minnesota; S. Battersby, *New Scientific* **2714**, (2009); M. Sambridge, H. Tkalcic, and A. Jackson, *Geo. Res. Lett.* **37**, L22301 (2010); G.K. Birajdar and V.H. Mankar, *Digital Investigation* **10**, 226 (2013).
 [5] A. Sen(De) and U. Sen, *Europhys. Lett.* **95**, 50008 (2011).
 [6] R.S. Pinkham, *Ann. Math. Stat.* **32**, 1223 (1961); T.P. Hill, *Am. Math. Mon.* **102**, 322 (1995); *Proc. Am. Math. Soc.* **123**, 887 (1995); *Stat. Sci.* **10**, 354 (1995); *Am. Sci.* **86**, 358 (1998).
 [7] J.J. Binney, N.J. Dowrick, A.J. Fisher, and M.E.J. Newman, *The Theory of Critical Phenomena: An Introduction to the Renormalization Group* (Clarendon, Oxford) (1992).
 [8] S. Sachdev, *Quantum Phase Transitions* (Cambridge University Press, Cambridge, 2011).
 [9] E. Lieb, T. Schultz, and D. Mattis, *Ann. Phys. (N.Y.)* **16**, 407 (1961); P. Pfeuty, *Ann. Phys. (N.Y.)* **57**, 79 (1970).
 [10] E. Barouch, B.M. McCoy, and M. Dresden, *Phys. Rev. A* **2**, 1075 (1970).
 [11] E. Barouch and B.M. McCoy, *Phys. Rev. A* **3**, 786 (1971).
 [12] R. Coldea, D. A. Tennant, E. M. Wheeler, E. Wawrzynska, D. Prabhakaran, M. Telling, K. Habicht, P. Smeibidl, and K. Kiefer, *Science* **327**, 177 (2010).
 [13] R. Islam, E.E. Edwards, K. Kim, S. Korenblit, C. Noh, H. Carmichael, G.-D.Lin, L.-M. Duan, C.-C. Joseph Wang, J.K. Freericks, and C. Monroe, *Nature Commun.* **2**, 377 (2011), and references therein.
 [14] A. Bhattacharya, *Bull. Calcutta Math. Soc.* **35**, 99 (1943).
 [15] H.-Q. Zhou, H.-H. Zhao, and B. Li, *J. Phys. A: Math. Theor.* **41**, 492002 (2008).
 [16] A. Osterloh, L. Amico, G. Falci, and R. Fazio, *Nat. Phys.* (416), 608 (2001); T.J. Osborne and M.A. Nielsen, *Phys. Rev. A* **66**, 032110 (2002).
 [17] A. Biswas, A. Sen (De), and U. Sen, *Phys. Rev. A* **89**, 032331 (2014).
 [18] V.E. Korepin, N.M. Bogoliubov, and A.G. Izergin, *Quantum Inverse Scattering Method and Correlation Functions* (Cambridge University Press, Cambridge) (1993).
 [19] S. Sachdev and A.P. Young, *Phys. Rev. Lett.* **78**, 2220 (1997).